Journal of Zhejiang University SCIENCE A
ISSN 1673-565X (Print); ISSN 1862-1775 (Online)
www.zju.edu.cn/jzus; www.springerlink.com
E-mail: jzus@zju.edu.cn

Using interacting multiple model particle filter to track airborne targets hidden in blind Doppler*

DU Shi-chuan, SHI Zhi-guo†‡, ZANG Wei, CHEN Kang-sheng

(*Department of Information and Electronic Engineering, Zhejiang University, Hangzhou 310027, China*)

†E-mail: shizg@zju.edu.cn

Received Mar. 1, 2007; revision accepted June 18, 2007

Abstract: In airborne tracking, the blind Doppler makes the target undetectable, resulting in tracking difficulties. In this paper, we studied most possible blind-Doppler cases and summed them up into two types: targets' intentional tangential flying to radar and unintentional flying with large tangential speed. We proposed an interacting multiple model (IMM) particle filter which combines a constant velocity model and an acceleration model to handle maneuvering motions. We compared the IMM particle filter with a previous particle filter solution. Simulation results showed that the IMM particle filter outperforms the method in previous works in terms of tracking accuracy and continuity.

Key words: Interacting multiple model, Particle filter, Blind Doppler

doi: 10.1631/jzus.2007.A1277 **Document code:** A **CLC number:** TN911.72

INTRODUCTION

In airborne radar tracking, when the target flies tangentially with respect to the tracking radar, the reflected Doppler frequency from the target will become indiscriminate to the receiving radar, and the range-rate (or Doppler speed) of that flight may possibly be lower than the blind Doppler limit, i.e., the least range-rate the radar can measure. During the blind Doppler, there is no gated observation from the radar and this could last till the track is lost.

Although no tracking can be executed during the blind Doppler, the blind Doppler cannot always be maintained by the target and it has to reappear finally. Therefore, it is required that tracking should be resumed as soon as the radar detects the target again. The extended Kalman filter (EKF) is a competent technique for tracking with mild nonlinearity (Gordon and Ristic, 2002; Ristic *et al*., 2004), but this method is incapable of resuming tracking due to the blind Doppler's great nonlinearity. Preferred means are the particle filter (Arulampalam *et al*., 2002; Ristic *et al*., 2004; Zang *et al*., 2007) and the combined Kalman/particle filter, which can resume tracking very quickly by exploiting the prior knowledge of the blind zone (Gordon and Ristic, 2002; Zaugg *et al*., 2003).

A major difficulty of using constant velocity (CV) motion model for this issue lies in the target's maneuverability which specifically refers to the varying extent of the blind Doppler region (existing period and area) and accelerations before the target's hiding and after its reappearance. The methods in (Gordon and Ristic, 2002; Zaugg *et al*., 2003) may have difficulties in dealing with such maneuverability. Multiple model method is a main trend of dealing with high maneuver motions. (Li and Jilkov, 2005). Therefore, in this paper, based on previous work in (Gordon and Ristic, 2002), we borrowed the main ideas of the interacting multiple model particle filter proposed by Boers and Driessen (2003) to improve the filtering (Blom and Bar-Shalom, 1988; Boers and Driessen, 2003). Despite the fact that interacting

‡ Corresponding author

* Project supported by China Postdoctoral Science Foundation (No. 20060400313) and partly by Zhejiang Postdoctoral Science Foundation of China (No. 2006-bsh-25)

multiple model method enhances system complexity, it requires fewer particles than single CV model to obtain the same or better performance.

The rest of this paper is organized as follows. Section 2 describes the movement model. Section 3 introduces the generalized types of the blind Doppler. Section 4 describes the algorithm of the interacting multiple model particle filter, and Section 5 presents the simulation results. Finally we conclude the paper.

MOVEMENT MODEL

The movement is described efficiently by two models: CV model and the acceleration model. We do not know the true acceleration beforehand, therefore a specified process noise is added to make the acceleration adjust itself. The detail will be discussed later.

The state dynamics are:

$$\boldsymbol{x}_{k+1}=F(\boldsymbol{x}_k,T_k,m)+\Gamma(T_k,m)\boldsymbol{v}_k(m), \quad (1)$$

where m={1,2}. m=1 corresponds to the CV model, and m=2 corresponds to the acceleration model. State evolutions of the two modes are given below:

$$F(\boldsymbol{x}_k,T_k,1)=\begin{bmatrix}1 & T_k & 0 & 0\\ 0 & 1 & 0 & 0\\ 0 & 0 & 1 & T_k\\ 0 & 0 & 0 & 1\end{bmatrix}\boldsymbol{x}_k,\ \text{with}\ \boldsymbol{x}_k=\begin{bmatrix}x_k\\ v_{x_k}\\ y_k\\ v_{y_k}\end{bmatrix},$$

and $\Gamma(T_k,1)=\begin{bmatrix}a_{\mathrm{s}}T_k^2/2 & 0\\ a_{\mathrm{s}}T_k & 0\\ 0 & a_{\mathrm{s}}T_k^2/2\\ 0 & a_{\mathrm{s}}T_k\end{bmatrix}$ for mode 1;

$$F(\boldsymbol{x}_k,T_k,2)=\begin{bmatrix}1 & T_k & T_k^2/2 & 0 & 0 & 0\\ 0 & 1 & T_k & 0 & 0 & 0\\ 0 & 0 & 1 & 0 & 0 & 0\\ 0 & 0 & 0 & 1 & T_k & T_k^2/2\\ 0 & 0 & 0 & 0 & 1 & T_k\\ 0 & 0 & 0 & 0 & 0 & 1\end{bmatrix}\boldsymbol{x}_k,$$

with state $\boldsymbol{x}_k=\begin{bmatrix}x_k & v_{x_k} & a_{x_k} & y_k & v_{y_k} & a_{y_k}\end{bmatrix}^{\mathrm{T}}$,

and $\Gamma(T_k,2)=\begin{bmatrix}a_{x_{\mathrm{m}}}T_k^2/2 & 0\\ a_{x_{\mathrm{m}}}T_k & 0\\ a_{x_{\mathrm{m}}} & 0\\ 0 & a_{y_{\mathrm{m}}}T_k^2/2\\ 0 & a_{y_{\mathrm{m}}}T_k\\ 0 & a_{y_{\mathrm{m}}}\end{bmatrix}$ for mode 2.

$T_k=t_{k+1}-t_k$, and $\boldsymbol{v}_k(1)$ is a 2×1 white Gaussian noise vector with covariance matrix $\boldsymbol{Q}(T_k)=\sigma_v^2\boldsymbol{I}_{2\times2}$. $\boldsymbol{v}_k(2)$ is 2×1 uniformly distributed noise, while $a_{x_{\mathrm{m}}}$ and $a_{y_{\mathrm{m}}}$ are set to be the maximum acceleration along x-axis and y-axis respectively. This process noise for mode 2 can handle acceleration maneuverability from zero to maximum acceleration, as remarked by Boers and Driessen (2003).

The measurement equation is

$$z_k=h(\boldsymbol{x}_k)+\boldsymbol{w}_k, \quad (2)$$

where $z_k=[X_k,\ Y_k,\ rr_k]^{\mathrm{T}}$ consists of position and range-rate measurements X_k, Y_k, rr_k. The unbiased conversions of measurements from polar coordinate to Cartesian coordinate are given by $X_k=\lambda^{-1}r_k\cos\theta_k$, $Y_k=\lambda^{-1}r_k\sin\theta_k$, with $\lambda=\exp(-\sigma_\theta^2/2)$ being the bias compensation factor (Mo *et al*., 1998). σ_r, σ_{rr} and σ_θ are the standard deviation for range, range-rate and azimuth respectively.

Measurement noise $\boldsymbol{w}_k$ is a 3×1 zero-mean Gaussian vector with covariance matrix

$$\boldsymbol{R}_k=\begin{bmatrix}\sigma_{X_k}^2 & \sigma_{X_kY_k}^2 & 0\\ \sigma_{X_kY_k}^2 & \sigma_{Y_k}^2 & 0\\ 0 & 0 & \sigma_{rr_k}^2\end{bmatrix}, \quad (3)$$

$\boldsymbol{v}_k$ and $\boldsymbol{w}_k$ are assumed to be independent.

The nonlinear function is defined as

$$h(\boldsymbol{x}_k)=\begin{bmatrix}x_k & y_k & \dfrac{x_kv_{x_k}+y_kv_{y_k}}{\sqrt{x_k^2+y_k^2}}\end{bmatrix}^{\mathrm{T}}. \quad (4)$$

The position variances and their cross-covariance are (Mo *et al*., 1998)

$$\begin{cases}\sigma_{X_k}^2 = (\lambda^{-2}-2)r_k^2\cos^2\theta_k + (r_k^2+\sigma_k^2)(1+\lambda^4\cos 2\theta_k)/2,\\ \sigma_{Y_k}^2 = (\lambda^{-2}-2)r_k^2\sin^2\theta_k + (r_k^2+\sigma_k^2)(1+\lambda^4\cos 2\theta_k)/2,\\ \sigma_{X_kY_k}^2 = (\lambda^{-2}-2)r_k^2\cos\theta_k\sin\theta_k + (r_k^2+\sigma_k^2)\lambda^4\cos 2\theta_k/2,\end{cases} \quad (5)$$

The detection probability is according to

$$P_{\mathrm{D}}(x_k) = \begin{cases} P_{\mathrm{d}}, \text{ if } \left|(x_k v_{x_k} + y_k v_{y_k})\big/\sqrt{x_k^2+y_k^2}\right| \ge L_{\mathrm{o}},\\ 0, \qquad \text{else,}\end{cases} \quad (6)$$

where L_{o} is the blind Doppler limit, and P_{d} is set to a number less than unity (Gordon and Ristic, 2002).

CASE STUDY

Under the constant velocity movement premise, there are two typical types of blind Doppler. Type I is intended tangential flying, and Type II is unintended flying leading to the blind Doppler as illustrated in Fig.1. Their true range-rate tracks are shown in Fig.2.

In Type I, starting with constant velocity motions for 30 s, the target makes a 3*g* (Gravity acceleration, g=9.81 m/s^2) turn, reappearing from the blind zone by the second 3*g* turn 15 s later, flies at the original velocity for 10 s and makes the third 3*g* turn. Twenty seconds later it reappears at the original velocity. In the whole 120-s flight, the target intends to make two blind Doppler zones as indicated in Fig.1a.

In Type II, the target flies at a constant velocity for 100 s. The absolute value of the range-rate is lower than the blind Doppler limit L_{o} for about 10 s because of large tangential velocity.

ALGORITHM OF INTERACTING MULTIPLE MODEL PARTICLE FILTER

To best highlight the blind Doppler, the target movement in unrestricted area (all areas except for the blind Doppler area) is not our main concern, but the period before it enters the blind Doppler (a transition from unrestricted area to the blind Doppler area) and the period after it reappears (transitions from the blind Doppler area to unrestricted area) are the decisive stages that ensure tracking continuity. Therefore, this algorithm aims at tracking the turns which can be detected and gated in Type I.

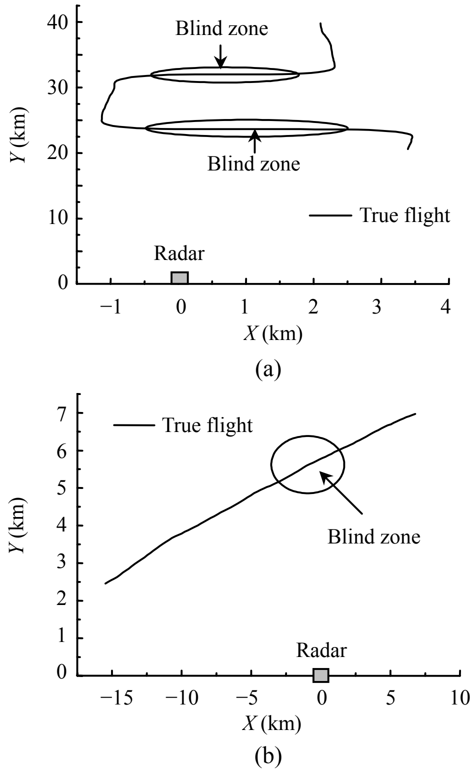

Fig.1 Flight track of Type I (a) and Type II (b)

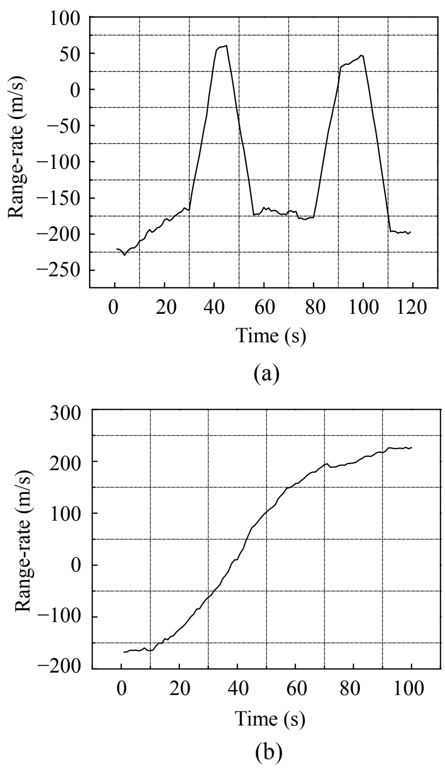

Fig.2 Range-rate of the flight. (a) Type I; (b) Type II

Let $\boldsymbol{x}_k^1(n)$ and $\boldsymbol{x}_k^2(n)$ (n=1, …, N) denote the particles for mode 1 and mode 2 respectively, and $\boldsymbol{x}_k^{\mathrm{BZ}}(n)$ (n=1, …, 2N) denote the blind zone particles. Mode transition probability is a Markov chain described as $p_{ij}=p\{m(k+1)=j|m(k)=i\}$.

The IMM particle filter algorithm is given below:

Initialization: *k*=1.

Draw sample $\boldsymbol{x}_k^1(n)$, $\boldsymbol{x}_k^2(n)$ from $p(\boldsymbol{x}_1)$. Set $p_1^{\mathrm{BZ}}=0$.

k=2, 3, …

(1) If $P_{\mathrm{d}}>0$ and $p_{k-1}^{\mathrm{BZ}}==0$, this means the target is detected and was in unrestricted area in previous sample time.

Interaction stage (mixing input):

$i, j\in m=\{1, 2\}$.

Mixing probabilities:

$$\mu_{i|j}(k-1\,|\,k-1)=p_{ij}\mu_i(k-1)/c_j,\ c_j=\sum_{i\in m}p_{ij}\mu_i(k-1).$$

A priori probability density for drawing samples $\hat{\boldsymbol{x}}_{k-1}^j(n)$:

$$\hat{p}_0^j(\boldsymbol{x}_{k-1}^{0j}\,|\,\boldsymbol{Z}_{k-1})=\sum_{i\in m}\hat{p}^i(\boldsymbol{x}_{k-1}^i\,|\,\boldsymbol{Z}_{k-1})\mu_{i|j}(k-1\,|\,k-1).$$

where $\boldsymbol{Z}_{k-1}$ is measurement sequence $\{\boldsymbol{z}_1, …, \boldsymbol{z}_{k-1}\}$.

Filtering stage:

Predicted samples:

$$\boldsymbol{x}_k^i(n)=F[\hat{\boldsymbol{x}}_{k-1}^i(n),T_{k-1},i]+\Gamma(T_{k-1},i)\boldsymbol{v}_{k-1}(i).$$

Probability weights: $w_k^i(n)\propto p[\boldsymbol{z}_k\,|\,\boldsymbol{x}_k^i(n)]$.

Normalised weights: $w_k^i(n)=\sum_{n=1}^{N}w_k^i(n)$.

Mean of samples: $\overline{\boldsymbol{x}}_k^i=\sum_{n=1}^{N}\boldsymbol{x}_k^i(n)w_k^i(n)$.

Covariance of samples:

$$P_k^i=\sum w_k^i[\overline{\boldsymbol{x}}_k^i-\boldsymbol{x}_k^i(n)][\overline{\boldsymbol{x}}_k^i-\boldsymbol{x}_k^i(n)]^{\mathrm{T}}.$$

Probability density formed by a sum of N weighted Gaussian densities:

$$\hat{p}^i(\boldsymbol{x}_k^i\,|\,\boldsymbol{Z}_k)=\sum_{n=1}^{N}w_k^i(n)N[\boldsymbol{x}_k^i(n),\upsilon_iP_k^i],$$

where $\upsilon_i=0.5N^{-2/d_i}$, d_i is the dimension of the state vector (Boers and Driessen, 2003).

Predicted output: $\boldsymbol{z}_k^i(n)=h[\boldsymbol{x}_k^i(n)]+w_k$.

Mean of predicted output: $\overline{\boldsymbol{z}}_k^i=\sum_{i=1}^{N}w_k^i(n)\boldsymbol{z}_k^i(n)$.

Residual covariance:

$$S_k^i=\sum_{n=1}^{N}\{h[\boldsymbol{x}_k^i(n)]-\overline{\boldsymbol{z}}_k^i\}\{h[\boldsymbol{x}_k^i(n)]-\overline{\boldsymbol{z}}_k^i\}^{\mathrm{T}}.$$

Innovations: $\boldsymbol{r}_k^i=\boldsymbol{z}_k-\overline{\boldsymbol{z}}_k^i$.

Likelihoods: $L_k^i=N(\boldsymbol{r}_k^i;0,S_j^i)$.

Mode probabilities: $\mu_k^i=L_k^ic_i/c,\ c=\sum_{i\in m}L_k^ic_i$.

Set $p_k^{\mathrm{BZ}}=0$.

Combined output stage: $\overline{\boldsymbol{x}}_k=\sum_{i\in m}\mu_i\overline{\boldsymbol{x}}_k^i$.

(2) If $P_{\mathrm{d}}>0$ and $p_{k-1}^{\mathrm{BZ}}==1$, this means the target is detected but was in blind area in previous sample time.

Set mode probability to $\mu_i=0.5$.

Evolve blind particles using mode 1 (assuming only CV motions in blind zone)

$$\boldsymbol{x}_k^{\mathrm{BZ}}(n)=F[\boldsymbol{x}_{k-1}^{\mathrm{BZ}}(n),T_{k-1},1]+\Gamma(T_{k-1},1)\boldsymbol{v}_k(1).$$

Generate $\boldsymbol{x}_k^1(n)$, $\boldsymbol{x}_k^2(n)$ from $\boldsymbol{x}_k^{\mathrm{BZ}}(n)$ with the largest weights (That means selecting N particles with the top N weights from the 2N blind-zone particles).

Next, implement the filtering stage, starting from the "Normalised weights" step.

(3) If $P_{\mathrm{d}}==0$ and $p_{k-1}^{\mathrm{BZ}}==0$, this means the target is in blind area but was in unrestricted area in previous sample time.

$\boldsymbol{x}_{k-1}^{\mathrm{BZ}}(n)$ are generated from the resampling of $\boldsymbol{x}_{k-1}^1(n)$, $\boldsymbol{x}_{k-1}^2(n)$ using the resampling method in (Ristic *et al.*, 2004).

Evolve particles (assuming only CV motions in blind zone)

$$\boldsymbol{x}_k^{\mathrm{BZ}}(n)=F[\boldsymbol{x}_{k-1}^{\mathrm{BZ}}(n),T_{k-1},1]+\Gamma(T_{k-1},1)\boldsymbol{v}_{k-1}(1).$$

Set $p_k^{\mathrm{BZ}}=1$.

(4) If $P_{\mathrm{d}}==0$ and $p_{k-1}^{\mathrm{BZ}}==1$, this means the target is in blind area and was in blind area in previous sample time.

Evolve blind particles using mode 1 (assuming only CV motions in blind zone)

$$\boldsymbol{x}_k^{\mathrm{BZ}}(n)=F[\boldsymbol{x}_{k-1}^{\mathrm{BZ}}(n),T_{k-1},1]+\Gamma(T_{k-1},1)\boldsymbol{v}_k(1).$$

Set $p_k^{\mathrm{BZ}}=1$.

SIMULATION RESULTS

The simulations are carried out by Matlab. We compared the IMM particle filter with the particle filter in (Gordon and Ristic, 2002). We evaluated both filters' performance by average errors and track score S. The track score is defined by $S_k'=S_{k-1}+\delta^+$, $S_k=\min(S_k',1)$, if target detected and gated with the filter not losing the track; otherwise $S_k'=S_{k-1}-\delta^-$, $S_k=\max(S_k',0)$, where $\delta^+=0.02$, $\delta^-=0.03$.

The parameters used in simulations are: $\sigma_v=3$ m/s, $\sigma_r=5$ m, $\sigma_{rr}=5$ m/s and $\sigma_\theta=0.1$ rad. The sample interval $T_s=1$ s; the detection probability is $P_d=0.9$; $L_o=30$ m/s; and the target speed is 800 km/h. The maneuverability parameters are $a_s=5\sim10$ m/s^2, and $a_{x_m}=a_{y_m}=20$ m/s^2. The mode transition probability matrix is $\pi=\begin{bmatrix}0.95 & 0.05\\0.05 & 0.95\end{bmatrix}$.

Fig.3 and Fig.4 show the simulation results of

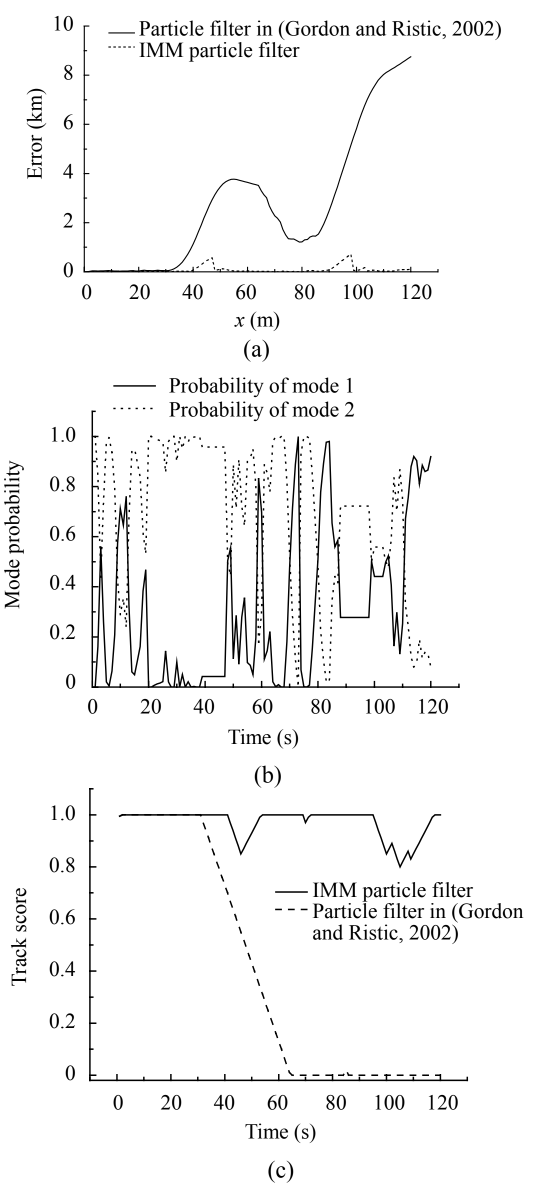

Fig.3 Comparison of IMM particle filter and particle filter proposed by Gordon and Ristic (2002). Simulation results of Type I. (a) Average position errors of 50 simulations; (b) Average mode probabilities of 50 simulations; (c) Track score

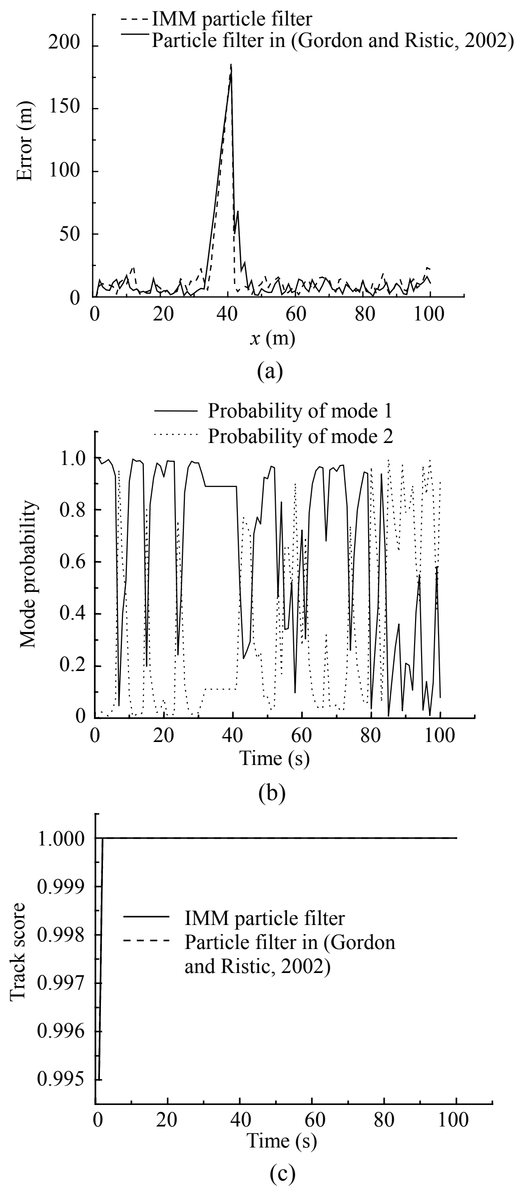

Fig.4 Comparison of IMM particle filter and particle filter proposed by Gordon and Ristic (2002). Simulation results of Type II. (a) Position errors; (b) Mode probability; (c) Track score

Type I and Type II, respectively. We use 1000 particles for IMM particle filter, 3000 particles for particle filter in (Gordon and Ristic, 2002) for Type I and 1000 for Type II.

The difference shown in Fig.3a is due to the fact that the IMM particle filter kept tracking for all the turning sections and thus stayed not far from the target when it was about to reappear. And the particle filter in (Gordon and Ristic, 2002) could not follow the target from the moment it entered the blind zone and thus failed to resume tracking at the reappearance of the target.

Fig.3b shows the mode probabilities roughly coincide with the target's true state of movement. Since the initial value of the acceleration in mode 2 is set to 0, there is quite a possibility that it would be effective for a short period during the constant velocity motion. This also happens in simulations for Type II, as shown in Fig.4b.

Fig.3c shows that IMM particle filter can maintain a track score not lower than 0.8, but the score of the other particle filter falls down to zero in the middle of the track period.

Fig.4 shows that the IMM particle filter has comparable performance with the one in (Gordon and Ristic, 2002) for Type II, because there is little maneuverability in the flight. In fact, Type II is a special case, because in reality most blind Doppler issues arise from maneuverable movements. In general, the IMM particle filter is more competent in dealing with uncertain situations (i.e. the blind Doppler issue) during a tracking than the particle filter using a single model.

CONCLUSION

In this work, we studied most cases of blind Doppler, and categorized them into two types: intentional tangential flying to the radar and unintentional flying that also leads to the blind Doppler. Enlightened by the work of (Boers and Driessen, 2003), we proposed an interacting multiple model particle filter which combines a constant velocity model and an acceleration model to handle maneuvering motions. We compared the IMM particle filter with the particle filter proposed by Gordon and Ristic (2002). Simulation results showed that the IMM particle filter outperforms the other method in terms of tracking accuracy and continuity.

References

Arulampalam, M.S., Maskell, S., Gordon, N., Clapp, T., 2002. A tutorial on particle filters for online nonlinear/ non-Gaussian Bayesian tracking. *IEEE Trans. on Signal Processing*, **50**(2):174-187. [doi:10.1109/78.978374]

Blom, A.P., Bar-Shalom, Y., 1988. The interacting multiple model algorithm for systems with Markovian switching coefficients. *IEEE Trans. on Automatic Control*, **33**(8): 780-783. [doi:10.1109/9.1299]

Boers, Y., Driessen, J.N., 2003. Interacting multiple model particle filter. *IEE Proc. RSN*, **150**(5):344-349.

Gordon, N.J., Ristic, B., 2002. Tracking airborne targets occasionally hidden in the blind Doppler. *Digital Signal Processing*, **12**:383-393. [doi:10.1006/dspr.2002.0439]

Li, X.R., Jilkov, V.P., 2005. Survey of maneuvering target tracking. Part V: Multiple-model methods. *IEEE Trans. on Aero. Electr. Syst.*, **41**(4):1255-1321. [doi:10.1109/TAES.2005.1561886]

Mo, L.B., Song, X.Q., Zhou, Y.Y., Sun, Z.K., Yaakov, B., 1998. Unbiased converted measurements for tracking. *IEEE Trans. on Aero. Electr. Syst.*, **34**(3):1023-1027. [doi:10.1109/7.705921]

Ristic, B., Arulampalam, S., Gordon, N., 2004. Beyond the Kalman Filter: Particle Filter for Tracking Applications. Artech House.

Zang, W., Shi, Z.G., Du, S.C., Chen, K.S., 2007. Novel roughening method for reentry vehicle tracking using particle filter. *J. Electromagn. Waves & Appl.*, **21**(14): 1969-1981.

Zaugg, D.A., Samuel, A.A., Waagen, D.E., Schmitt, H.A., 2003. A Combined Particle/Kalman Filter for Improved Tracking of Beam Aspect Targets. IEEE Workshop on Statistical Signal Processing, p.535-538. [doi:10.1109/SSP.2003.1289512]